GRADIENT ARTEFACT CORRECTION IN THE EEG SIGNAL RECORDED WITHIN THE fMRI SCANNER

José L. Ferreira[1], Pierre J. M. Cluitmans[1] and Ronald M. Aarts[1,2]
[1]*Department of Electrical Engineering, Eindhoven University of Technology, Eindhoven, The Netherlands*
[2]*Philips Research Laboratories Eindhoven, Eindhoven, The Netherlands*
{j.l.ferreira, p.j.m.cluitmans, r.m.aarts}@tue.nl

Keywords: Combined EEG-fMRI, Imaging artefact correction, Average artefact subtraction, Artefact template variability modelling.

Abstract: In recent years, combined EEG-fMRI has become a powerful brain imaging technique which is largely employed in clinical and neuroscience research. Parallel to the achievements reached in this area, a number of challenges remain to be overcome in order to consolidate such technique as an independent and effective method for brain imaging. In particular, the occurrence of gradient artefacts in the EEG signal due to the magnetic field of the fMRI magnetic scanner. This paper presents a proposal for modelling the variability of the gradient artefact template which makes use of the standard deviation and the slope differentiator between consecutive samples of the signals. Combination of such a model with the average artefact subtraction method achieves a reasonable elimination of the gradient artefact from EEG recordings.

1 INTRODUCTION

Combined EEG-fMRI (acquisition of electroencephalogram during functional magnetic resonance imaging) is a technique for multimodal brain activity mapping that has got a broad usage for research and clinical purposes (Villringer et al., 2010). Ritter and Villringer (2006) reinforce that co-registered EEG-fMRI has attracted the interest of several researchers and clinicians last years and it has revealed itself a promising and additional monitoring tool of the human brain activity.

Gonçalves et al. (2007) mention that although such a brain imaging technique was first applied in the field of epilepsy, nowadays it has been extended to other types of neuroscience studies and applications. Villringer et al. (2010) mention that only simultaneous EEG-fMRI offers the opportunity to relate both brain imaging modalities to actual brain events, a characteristic which is relevant for solving numerous research questions in basic and cognitive neuroscience.

Parallel to the breakthroughs achieved by using simultaneous combination of EEG-fMRI as an independent brain imaging technique, some problems related to its use remain to be solved in order to consolidate and to enable broadening its applications range. That is the case of the occurrence of artefacts in the EEG signal caused by the variation of the magnetic fields of the fMRI scanner, the so-called "gradient" or "imaging acquisition" artefact (Mulert and Hegerl, 2009).

2 OBJECTIVES

Gradient artefacts completely obscure the EEG, as illustrated in figure 1. According to Ritter et al. (2010), this type of artefact occurs in the EEG signal due to the voltage induced by the application of rapidly varying magnetic field gradients for spatial encoding of the MR signal and radiofrequency pulses (RF) for spin excitation in the circuit formed by the electrodes, leads, patient and amplifier.

The waveform of the gradient artefact caused by one RF pulse is approximately the differential waveform of the corresponding RF pulse. Imaging acquisition artefacts have amplitudes that can be several orders of magnitude higher than the neuronal EEG signal. Artefact amplitudes associated to the gradient switching (10^3 to 10^4 μV) are generally much larger than those arising from RF pulses (up to 10^2 μV) (Ritter et al., 2010).

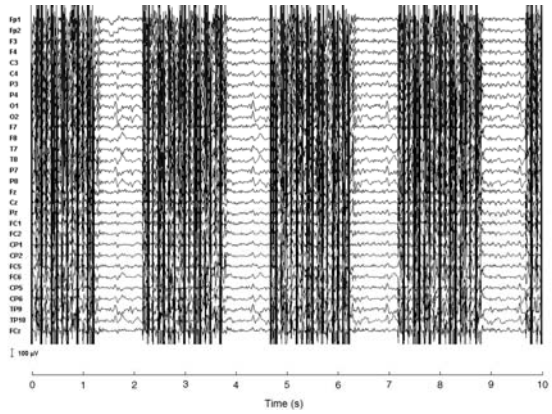

Figure 1: Imaging artefact in ongoing EEG data. Adapted from Mantini et al. (2007).

As discussed by Ritter et al. (2010), the frequency range of the gradient artefact exceeds that of standard clinical EEG, nevertheless the EEG recording is dominated by harmonics of the repetitive slice convolved with harmonics in the range of frequency of the volume repetitive frequency. The frequency of these harmonics overlaps the range frequency of the EEG signal. Moreover, also as mentioned by Ritter et al., such artefacts have a strong deterministic component because the preprogrammed nature of RF and gradient switching.

In literature, some techniques are suggested in order to attempt minimizing the effects of gradient artefacts in the EEG signal. For example, it is possible to reduce their magnitude at the source by laying out, immobilising and twisting the EEG leads, using a bipolar electrode configuration and using a head vacuum cushion. Further, depending on the application, a periodic interleaved approach, whereby the MR signal acquisition is suspended at regular intervals, could be used as well (Ritter et al., 2010).

Gonçalves et al. (2007) mention that concerning continuous MR acquisition, dedicated software solutions have to be developed in order to correct gradient artefacts in the electroencephalogram. Some post-processing signal methods for correction of gradient artefacts in the EEG signal are based upon time or frequency domain analysis which make use of different mathematical and computational digital signal processing approaches like spectrum analysis, principal component analysis, independent component analysis and average artefact subtraction (Gonçalves et al., 2007).

According to Allen et al. (2000), the average artefact subtraction methodology consists of the calculation of an average imaging artefact waveform or template over a fixed number of samples, and it is then subtracted from the EEG signal for each sample.

Performing average artefact subtraction alone does not result to satisfactory quality of corrected signal, demanding the need for further residuals correction (Allen et al., 2000; Gonçalves et al., 2007). These authors also propose the use of adaptive noise cancelling for attenuating the remaining residuals from the subtraction by using low-pass filters, smoothing and downsampling. However, according to Van de Velde et al. (1998), the use of filtering could result in removing original component frequencies of the EEG signal.

The objectives of the current paper are to present an alternative approach for cleaning up such residuals by employing a specific model for evaluating and quantifying the variability of the imaging artefact. The proposed methodology is based upon information about the variance of the averaged template artefact as well as on the slope differentiator of the EEG signals under analysis.

3 MATERIALS AND METHODS

3.1 Features of the Data under Analysis

Simultaneous EEG and fMRI data were collected for a research focused on epilepsy and post-traumatic stress disorder (PTSD), jointly developed by the department of Psychiatry of Universiteit Medisch Centrum Utrecht, the Research Centre Military Mental Health Care in the Dutch Central Military Hospital in Utrecht and the Department of Research and Development of the Epilepsy Center of Kempenhaeghe in Heeze (The Netherlands).

Data were recorded from patients characterized as military veterans with PTSD which were in mission abroad through the outpatient clinic of the Military Mental Health Care. All participants were male and aged between 18 and 60 years.

3.2 Protocol for EEG-fMRI Data Collection

Functional magnetic resonance imaging scanning was carried out using a 3 T Scanner (Philips, Eindhoven, The Netherlands) at Kempenhaeghe Epilepsy Center. An MRI-compatible 64 channel polysomnograph was used to collect one ECG channel, two EOG channels, one EMG and 60 EEG

channels. In the current work, the ECG signal was used for synchronization purposes. EEG electrodes positioning was in accordance with the international 10-20 system electrodes placement.

EEG-fMRI data were collected during 45 minutes, before the period that the patient should sleep. After application of the EEG cap, the subjects were scanned using a functional echo-planar imaging sequence with 33 transversal slices (thickness 3 mm, TE 30 ms, TR 2500 ms).

The used electroencephalogram device for collecting the EEG signals possesses an appropriate built-in notch filter. The sampling rate for signal acquiring was 2048 Hz.

3.3 General Average Artefact Subtraction Overview

The basic idea of the average subtraction approach consists of estimating an average template of the gradient artefact along an observed range of the EEG signal, and then subtracting this template from the electroencephalogram at those regions where the artefact occurs (Allen et al., 2000). The average artefact subtraction can be described by the following expression:

$$\widehat{EEG}_{corct,i} = EEG_{raw,i} - \Gamma_{i-i_s}, \qquad (1)$$

where i runs over the number of samples within the entire EEG data set; i-i_s is the time sample along the selected EEG segments considered for average; $\mathbf{E\hat{E}G_{corct}}$ and $\mathbf{EEG_{raw}}$ are respectively the corrected and the uncorrected (raw) EEG signals; and $\mathbf{\Gamma}$ is the template to be subtracted.

According to the methodology proposed by Allen et al. (2000) to calculate such a template, the $\mathbf{EEG_{raw}}$ is divided in segments of fixed length (S number of samples). The resulting averaging from samples situated at the same segment position i-i_s corresponds to the template epoch Γ_{i-i_s}.

Allen et al. (2000) and Gonçalves et al. (2007) also consider the need for interpolation and extrapolation along the obtained fixed segment length. According to the approach for average gradient subtraction proposed by Gonçalves et al. (2007), interpolation is necessary since in general the clocks of the EEG and fMRI are uncalibrated and, in consequence, misaligned. Thus, a small time shift should be applied in order to compensate the misalignment and to eliminate the variation of the number of epochs among the slices segments.

Gonçalves et al. (2007) still take into account estimation of some parameters which must be computed before carrying out the artefact subtraction like the slice time (ST) and the dead time (DT) which are determined by minimizing a cost function that is related to the ratio between $\mathbf{E\hat{E}G_{corct}}$ and $\mathbf{EEG_{raw}}$.

3.4 Overview of the Average Artefact Subtraction Methodology Employed in this Work

In order to perform the estimation of the corrected EEG, $\mathbf{E\hat{E}G_{corct}}$, the model described in (1) was employed. In this sense, estimation of $\mathbf{\Gamma}$ was done by dividing the chosen range of the observed $\mathbf{EEG_{raw}}$ in segments with fixed length, as proposed by Allen et al. (2000) and Gonçalves et al. (2007). However, due to some specific features observed in the data analysed in the current work, a different approach to estimate the length of those segments was used.

Observation of the raw EEG data recorded during the MR scanning revealed that the slice length could be estimated by evaluation of the distance between typical peaks noticed in the raw EEG or ECG recordings that can be attributed to the magnetic fields switching within the MR scanner (Ritter et al., 2010). Figures 2 and 3 show the occurrence of those peaks in 2 s-segments of the raw EEG (electrode position F8) and raw ECG around the time instant 429.4 s.

It is important to highlight that estimation of such a distance from the EEG data recorded within the scanner was necessary since: i) the electromagnetic properties of different sources of the system constituted by the electroencephalograph, the fMRI scanner and patient have influence on the artefact generation and morphology; ii) that is the existing condition for the available data under analysis. Thereby, it could not be evaluated just by placing one electrode directly in the fMRI scanner.

Performing measurement of the distance between peaks by using such a procedure allowed to estimate the value of ST around (155 ± 1) epochs that correspond to a time interval of approximately (0.07568 ± 0.00050) s considering the data under analysis in this work.

Thus, as a first approach, the used segment length was the slice length itself, and EEG was divided in segments of 155 epochs, according to the measured distance between the peaks corresponding to the beginning of each MR slice. In the case of the segments that contained more or less than 155 epochs, extrapolation or interpolation were done in order to fix the length of the segments and therefore

to compensate the misalignment between the EEG and fMRI clocks (Gonçalves et al., 2007).

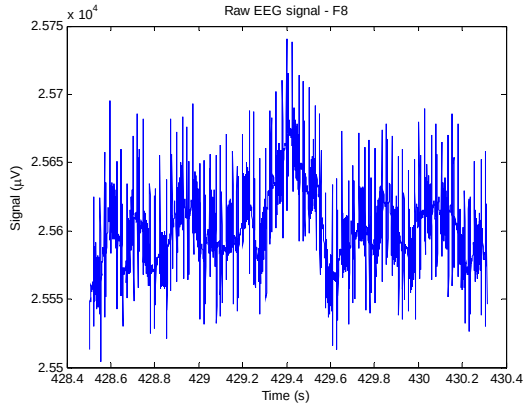

Figure 2: 2 s-segment around the time instant 429.4 s of the raw EEG signal (electrode position F8), showing the peaks caused by MR switching.

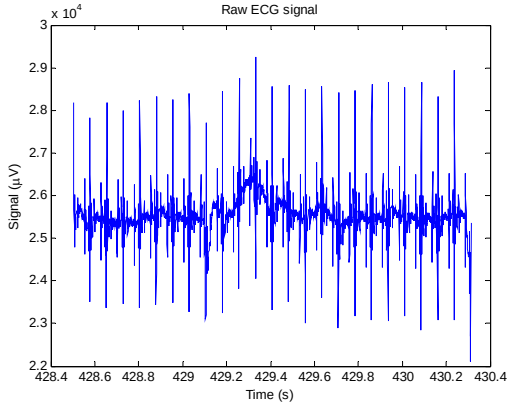

Figure 3: 2 s-segment around the time instant 429.4 s for the raw ECG signal, showing the peaks caused by MR switching.

The algorithm used for performing the average subtraction was adapted from Bishop (2006) and Press et al. (1992), and is based upon the idea that the mean of a random variable corresponds to the point where the random variable has the minimum variance. By this approach, epochs from the different segments in which the raw EEG was divided and have a corresponding position within the slice, $EEG_{raw,i,j}$, can be related to an initial choice for the template average epoch at the same slice position, $\mu_{i\text{-}i_s}$ (= Γ_{i-i_s}), by the following cost function:

$$\Psi_{i\text{-}i_s}(\mu_{i\text{-}i_s}) = \sum_{j=1}^{J} (EEG_{raw,i,j} - \mu_{i\text{-}i_s})^2 , \quad (2)$$

where J is the number of slices considered for averaging. The rationale for using this formula is that in addition to calculate the averaged gradient artefact template, minimization of (2) provides to estimate jointly the variance (standard deviation) associated to each epoch, parameter which is used during modelling and correction of the artefact variability as described in the next section. (2) can be rewritten into the following matrix format:

$$\Psi_{i\text{-}i_s}(\mu_{i\text{-}i_s}) = \mathbf{K}^{\mathbf{T}} \cdot \mathbf{K} , \quad (3)$$

where $\mathbf{K}$ is a vector with *Jx1* components $K_j = EEG_{raw,i,j} - \mu_{i\text{-}i_s}$. Therefore, the value of $\Psi_{i\text{-}i_s}$ is the variance associated to the template epoch i-i_s. Finally, the values of $\mathbf{E\hat{E}G_{corct}}$ (and $\mathbf{\Gamma}$) can be calculated from:

$$\mathbf{Z} = \mathbf{K} \cdot \mathbf{K}^{\mathbf{T}} . \quad (4)$$

The square root of the diagonal elements of $\mathbf{Z}$ corresponds to the values of $E\hat{E}G_{corct,i}$.

3.5 Modelling of Imaging Artefact Template Variability

For elimination of the remaining residuals in the $\mathbf{E\hat{E}G_{corct}}$, a specific model is proposed for attempting to quantify the artefact variability. The use of this alternative approach was preferred since, according to Van de Velde et al. (1998), the use of filtering, as is done for conventional residuals elimination, could also remove some original frequencies of the EEG signal. Furthermore, the remaining artefact residuals can be attributed to the template variability.

Klados et al. (2009) suggest the use of an adaptive method whereby it is possible to approximate the $\mathbf{E\hat{E}G_{corct}}$ to the true EEG. According to that methodology, the template variability is evaluated by multiplying each artefact template sample by an estimated factor $\hat{a}_i$, and then subtraction is processed as follows:

$$E\hat{E}G_{corct,i} = EEG_{raw,i} - \hat{a}_i \Gamma_{i-i_s} . \quad (5)$$

The expression above is an adaptive extension of (1) whose limit referred to the filter parameter $\hat{a}_i$ allows refining the value of $\mathbf{E\hat{E}G_{corct}}$:

$$\lim_{\hat{a}_i \to a_i} E\hat{E}G_{corct,i} = EEG_{corct,i} . \quad (6)$$

Therefore as far as the parameter $\hat{\mathbf{a}}$ is approached to the optimal value of the adaptive filter $\mathbf{a}$, the value of $\mathbf{E\hat{E}G_{corct}}$ tends to the true EEG.

In the current work, this method was further modified in such a way that **â** is changed to a new non-filter parameter **â'** and equations (5) and (6) become:

$$EEG_{corct,i} = E\hat{E}G_{corct,i} - \hat{a}'_i R_i, \quad (7)$$

where the product of the corresponding elements of the vectors **â'** and **R** acts as an initial estimation of the remaining residual in the EEG. Hence, (7) allows to calculate a refinement for the value of the corrected EEG by subtracting an estimation of the remaining residual from the corresponding unrefined value obtained for $\mathbf{E\hat{E}G_{corct}}$.

As the parameters **â'** and **R** should represent the variability of the gradient artefact, their estimation took into account specific properties of the raw, corrected signal and true EEG that are supposed to reflect that variability. The standard deviation associated to the averaged imaging artefact and the signal slope differentiator were chosen as the properties of the signals that represents the variability, the former was associated to **â'** and the latter to **R**.

Concerning the standard deviation associated to the averaged artefact, it is a natural choice since it is a measurement of the variability of a random variable around the mean (Papoulis and Pillai, 2002). According to the GUM (2008) the standard deviation (or the variance) also could be seen as a component of the uncertainty measurement associated with the estimated average, and therefore could be used for quantifying and correcting the lack of information about the variability of the random variable.

The choice of the slope differentiator is in accordance with Van de Velde et al. (1998) that describe such a signal parameter associated to the large signal magnitudes as being particularly useful for detection of the high-frequency properties of the muscle artefact. At the same way, by observing the EEG signals under analysis, it is noticed that high-frequency as well as large signal magnitudes can be attributed to the gradient artefact. Thereby, in our work, the slope variation is also used to identify the imaging acquisition artefact. Moreover, a new approach is proposed to quantify the variability making use of the signal slope as well, as described below.

In our approach, estimation of the parameter **R** is based upon the simple differentiation of $\mathbf{EEG_{raw}}$, $diff\,(\mathbf{EEG_{raw}})$, $\mathbf{E\hat{E}G_{corct}}$, $diff\,(\mathbf{E\hat{E}G_{corct}})$, and the artefact free EEG. An artefact free EEG interval could be obtained from the available data, from approximately the first 5 s of the recordings of each EEG channel, allowing estimating the corresponding values for the slope differentiator.

By analysing the artefact free interval, it could be observed that the maximum value of the slope differentiator of the true EEG is estimated around 15 μV/sample. The values observed for the same parameter, considering $\mathbf{EEG_{raw}}$ and $\mathbf{E\hat{E}G_{corct}}$, are usually much higher when compared to the true EEG in such a way that it allows identification of epochs as being artefact free or not, which is in accordance with the methodology proposed by Van de Velde et al. (1998). The values of the elements of **R** were quantified by taking into account the normalized values of $diff\,(\mathbf{E\hat{E}G_{corct}})$, whose maximum value was considered as being equal to 1, as follows:

$$R_{norm,i} = \frac{\left|(E\hat{E}G_{corct,i+1} - E\hat{E}G_{corct,i})\right|}{\max\left|diff\,(\mathbf{E\hat{E}G_{corct}})\right|}. \quad (8)$$

Thus, $R_{norm,i}$ corresponds to the normalized value of $diff\,(\mathbf{E\hat{E}G_{corct}})$.

As mentioned above, the elements of vector **â'** (i.e., $\hat{a}_i'$) were related to the value of standard deviation $\hat{s}_{i-i_s}$ of the gradient average artefact, as indicated in (9) and 10:

$$\hat{a}'_i = \hat{s}_{i-i_s}; \quad (9)$$

$\hat{s}_{i-i_s}$ is equal to the root square of the template variance:

$$\hat{s}_{i-i_s} = \sqrt{\Psi_{i-i_s}}. \quad (10)$$

Finally, considering (8), (9) and (10), expression (7) can be rewritten as:

$$EEG_{corct,i} = E\hat{E}G_{corct,i} - \hat{s}_{i-i_s} R_{norm,i}. \quad (11)$$

Therefore, the limit described in equation (6) is carried out by performing the subtraction indicated in (11) iteratively, until a predetermined threshold value is reached. In this work, the threshold was set as being the value of $diff\,(\mathbf{EEG_{corct}})$ coincident with the mean plus the standard deviation calculated for the slope differentiator of the true EEG (estimated around 1.5 μV/sample for the available data).

It is worthwhile to consider that in our approach the values of the parameter $R_{norm,i}$ act as weights varying from 0 to 1 which indicate what percentage of the standard deviation $\hat{s}_{i-i_s}$ should be applied for refinement of $E\hat{E}G_{corct,i}$. In other words, the value of $R_{norm,i}$ acts as an indicator of the presence of the gradient artefact in $\mathbf{E\hat{E}G_{corct}}$ (Van de Velde et al., 1998) and at the same time indicates the amount of correctness based on $\hat{s}_{i-i_s}$ that should be applied on $E\hat{E}G_{corct,i}$.

4 RESULTS

In figure 4, the artefact free 5 s-period of the raw EEG corresponding to the EEG at channel F8 is depicted. It is noticed that there is a DC offset in the signal around 2.55×10^4 μV. A similar DC component is also observed for the other electrode EEG positions and ECG recording.

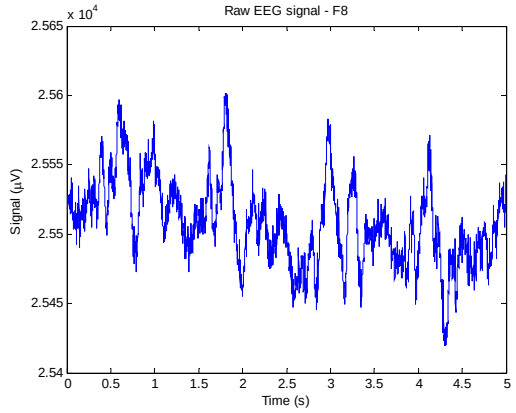

Figure 4: Artefact free period of raw EEG signal recording, corresponding to electrode position F8. A DC component around 2.55×10^4 μV can be observed.

In order to estimate the artefact template $\mathbf{\Gamma}$, a set of eight subsequent segments ($J = 8$ slices) were considered from the raw EEG signal. Figure 5 shows one set of slices picked up from the raw EEG signal already containing interpolated or extrapolated epochs depending on the need, and used during the calculations.

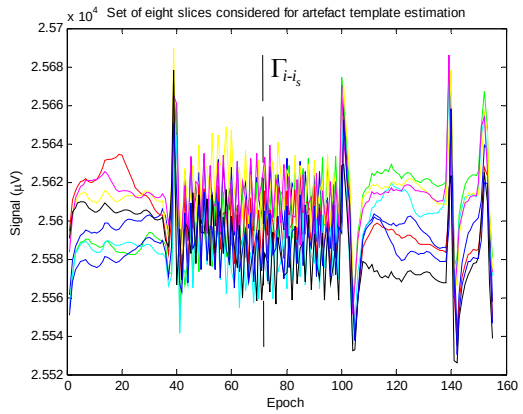

Figure 5: Set of eight ($J = 8$) subsequent EEG segments slice-length (155 epochs) around the time instant of 430 s considered for averaging. The average template $\mathbf{\Gamma}$ is calculated considering corresponding epochs of each segment (Allen et al., 2000).

Figure 6 shows the results of the average artefact subtraction described by application of equations (2), (3) and (4) on the raw EEG signal showed in figure 2. Nevertheless the observed DC component has been removed, in comparison to the artefact free EEG signal of figure 4, a considerable amount of remaining residual peaks uniformly distributed along the signal resulting from the gradient artefact are still observed in figure 6.

Hence, in order to obtain a better correction for $\mathbf{E\hat{E}G_{corct}}$, equations (8) to (11) are then applied to the signal of figure 6, resulting to the signal depicted in figure 7. From this figure, it could be seen that the noticed residuals in figure 6 were strongly cleaned up.

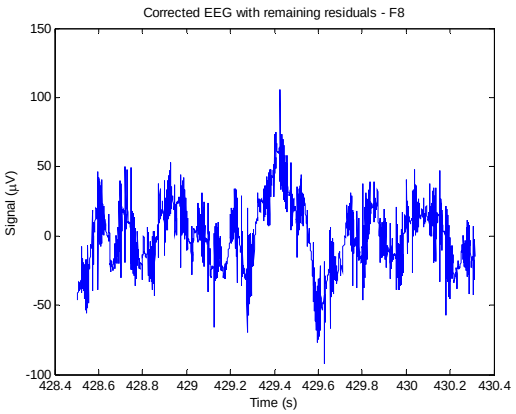

Figure 6: Signal resulting ($\mathbf{E\hat{E}G_{corct}}$) from application of equations (2), (3) and (4) on the signal of figure 2.

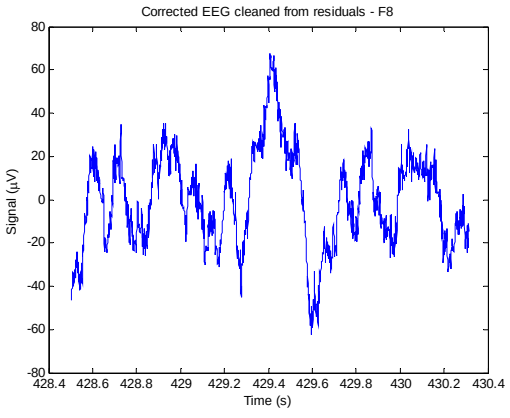

Figure 7: Signal resulting ($\mathbf{EEG_{corct}}$) from application of equations (8) to (11) on the signal of figure 6.

Finally, figures 8 and 9 depict zooming in (0.7 s-segment length) around the time instant 430 s, showing superposition of the signals raw EEG and $\mathbf{EEG_{corct}}$, and the signals $\mathbf{E\hat{E}G_{corct}}$ and $\mathbf{EEG_{corct}}$.

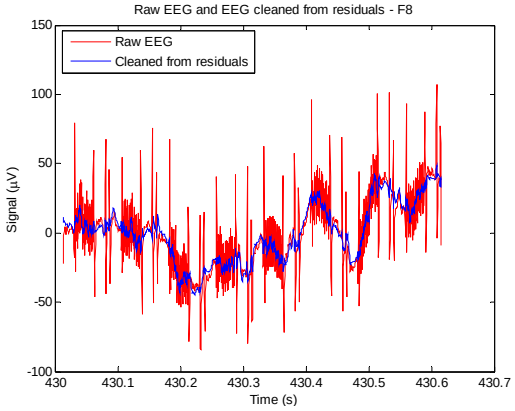

Figure 8: 0.7 s-segment around the time instant 430 s of the signal $\mathbf{EEG_{corct}}$ (cleaned from residuals) superimposed to the raw EEG (without DC offset).

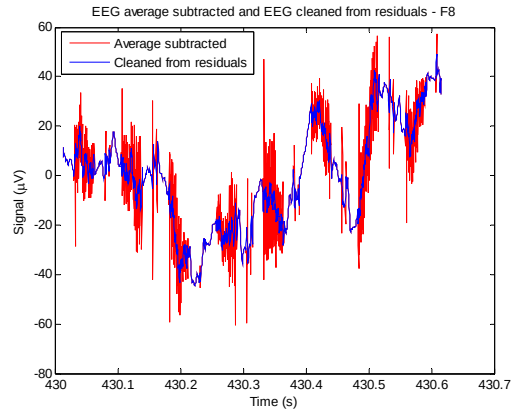

Figure 9: 0.7 s-segment around the time instant 430 s of the signal $\mathbf{EEG_{corct}}$ (cleaned from residuals) superimposed to $\mathbf{\hat{EEG}_{corct}}$ (average subtracted).

5 DISCUSSION

As can be regarded in figure 8 and 9, combination of the methods average artefact subtraction with the approach here proposed for cleaning up the resulting residuals from that subtraction have achieved a strong elimination of the gradient artefact from the raw EEG signal.

As regarded in figure 6, just the average artefact subtraction approach described in equations (2), (3) and (4) does not result to satisfactory elimination of the artefact from the EEG signal since a considerable amount of residuals remains in the resulting corrected signal (figure 6). Such residuals can be attributed to the variability of the imaging artefact and this information is not taken into account when only the average is used in the correction. Nevertheless the waveform of the gradient artefact possesses a strong deterministic (Ritter et al., 2010) and reproducible component, as could be noticed in figure 5, the variability associated with the artefact provokes the presence of residuals in the corrected EEG and, therefore, the need for further correction.

Hence, in our approach for removing the artefact residuals, it is proposed to use additional characteristics from the available data which could contain some information about the template variability as well as which could enable to quantify the magnitude of the residuals. The two chosen signal characteristics were the standard deviation associated to the averaged (Papoulis and Pillai, 2002; GUM, 2008) template and the signal slope differentiator (Van de Velde et al., 1998), and showed themselves fit those requirements since the use of equations (5) to (11) allows elimination of the residuals as is depicted in figure 7.

Therefore, combination of the average artefact subtraction method and the methodology for quantifying the variability of the template of the imaging artefact proposed here reveals itself to be an alternative method for cleaning up the EEG signal from the gradient artefact, which could produce a good quality for the resulting corrected signal. Nevertheless the model described in equations (5) to (11) constitutes a prototype and requires more accurate refinement and validation, some advantages of its application could be mentioned in comparison to other methods.

Firstly, the employed approach is implemented only in the time domain. In addition, it does not requires insertion of markers in the EEG signal since the value of important events associated to the MR scanning like ST, DT and TR could be evaluated directly from data (observed peaks in the raw signals caused by the imaging artefact). Furthermore, the entire estimation of the model parameters is based upon the use of simple statistical parameters of the signals like mean, standard deviation and mode. Another observed advantage of the employed methodology is that, in principle, a low number of slices could be used during template averaging without the need for using the slices of the entire MR volume as well as recordings from other EEG channels. This consideration could be useful in future developments concerning real time applications. Finally, in principle there is no need for using filtering; this fact will be evaluated in future steps for method validation.

The use of the synchronized ECG signal was useful during application of the proposed

methodology since the events related to the MR scanning occur simultaneously in the EEG and the ECG recordings, in such a way that the electrocardiogram can be used for estimation of relevant parameters associated to the proposed correction methodology which also are valid for the electroencephalogram.

6 CONCLUSIONS

A prototype model for quantifying the gradient template variability combined with the average artefact template subtraction methodology was applied for removing gradient artefact from EEG signals, and proves to be promising as an alternative approach for obtaining a good signal correction.

As described in literature (Allen et al., 2000; Gonçalves et al., 2007), the average artefact subtraction alone does not result to satisfactory quality of corrected signal, demanding the need for further residuals correction. As discussed by Van de Velde et al. (1998), the use of filtering could result in removing original component frequencies of the EEG signal. Therefore, in this work a model for identification and quantification of the residuals to be subtracted is proposed, instead the usual employment of low-pass filtering for cleaning up the remaining residuals.

In future work, the influence of a higher number of slices (for instance, the entire number of slices of the MR volume) must be checked as well as signal estimation of the time intervals corresponding to the dead time (DT) have to be carried out using the presented approach. Also, the proposed model has to be applied to a larger set of EEG clinical data in order to evaluate its consistency.

Finally, as an additional recommendation for future work, it should be analyzed if the proposed methodology could be extended for correction of other types of artefact as well as could be consolidated as an alternative average subtraction approach for signal correction.

ACKNOWLEDGEMENTS

We are grateful to Saskia van Liempt, M.D., and Col. Eric Vermetten, M.D., Ph.D. from the University Medical Center/Central Military Hospital, Utrecht, for providing the data presented in this work. This work has been made possible by a grant from the European Union and Erasmus Mundus – EBW II Project.

REFERENCES

Allen, P., Josephs, O., Turner, R., 2000. A method for removing imaging artefact from continuous EEG recorded during functional MRI. *NeuroImage.* 12. Elsevier: 230-239.

Bishop, C., 2006. *Pattern recognition and machine learning*. Springer: New York.

Gonçalves, S., Pouwels, P., Kuijer, J., Heethaar, R., de Munck, J., 2007. Artefact removal in co-registered EEG/fMRI by selective average subtraction. *Clinical Neurophysiology.* 118. Elsevier: 823-838.

GUM, 2008. *Evaluation of measurement data – Guide to the expression of uncertainty in measurement.* 1st ed. JCGM.

Klados, M., Papadelis, C., Bamidis, P., 2009. A new hybrid method for EOG artefact rejection. *9th International Conference on Information Technology and Application in Biomedicine, ITAB 2009, Larnaca, Cyprus, November 5-7, 2009, Proceedings:* 4937-4940.

Mantini, D., Perucci, M., Cugini, S., Romani, G., Del Gratta, C., 2007. Complete artefact removal for EEG recorded during continuous fMRI using independent component analysis. *NeuroImage.* 34. Elsevier: 598-607.

Mulert, C., Hegerl, U., 2009. Integration of EEG and fMRI. In E. Kraft, G. Gulyás, E. Pöppel (eds.), *Neural correlation of thinking.* Springer: Verlag, Berlin, Heidelberg.

Papoulis, A.; Pillai, S., 2002. *Probability, random variables, and stochastic processes.* 4th ed. New York: McGraw-Hill.

Press, W.; Teukolsky, S.; Vetterling, W; Flannery, B., 1992. *Numerical recipes in C*: the art of scientific computing. 2nd ed. Cambridge University Press: Cambridge.

Ritter, P., Becker, R., Freyer, F., Villringer, A., 2010. EEG quality: the image acquisition artefact. In C. Mulert, L. Limieux (eds.), *EEG-fMRI: Physiological basis, technique and applications.* Springer: Verlag, Berlin, Heidelberg.

Ritter, P., Villringer, A., 2006. Simultaneous EEG-fMRI. *Neuroscience and Biobehavioral Reviews.* 30. Elsevier: 823-838.

Van de Velde, R., Van Erp, G., Cluitmans, P., 1998. Detection of muscle artefact removal in the normal human awake EEG. *Electroencephalography and Clinical Neurophysiology.* 107. Elsevier: 149-158.

Villringer, A., Mulert, C., Lemieux, L., 2010. Principles of multimodal functional imaging and data integration. In C. Mulert, L. Limieux (eds.), *EEG-fMRI: Physiological basis, technique and applications.* Springer: Verlag, Berlin, Heidelberg.